Eur. Phys. J. B **11**, 75–81 (1999)

THE EUROPEAN PHYSICAL JOURNAL B

EDP Sciences

$TA_1[110]$ phonon dispersion and martensitic phase transition in ordered alloys Fe_3Pt

J. Kästner[1,a], J. Neuhaus[2], E.F. Wassermann[1], W. Petry[2], B. Hennion[3], and H. Bach[4]

[1] Labor für Tieftemperaturphysik and SFB 166, Gerhard-Mercator-Universität Duisburg, 47048 Duisburg, Germany
[2] Physik Department E13, Technische Universität München, 85747 Garching, Germany
[3] Laboratoire Léon Brillouin, CEA Saclay, 91191 Gif-sur-Yvette Cedex, France
[4] Institut für Experimentalphysik IV and SFB 166, Ruhr Universität Bochum, 44780 Bochum, Germany

Received 18 January 1999 and Received in final form 11 March 1999

Abstract. In a previous neutron scattering study, we had observed that the $TA_1[\xi\xi 0]$ phonon softening in $L1_2$-ordered ferromagnetic $Fe_{72}Pt_{28}$ Invar is pronounced at the zone boundary M-point and leads to an antiferrodistortive phase transition at low temperatures. Here, we report on similar neutron scattering investigations on two ordered crystals with higher Fe content to investigate the relation between the $TA_1[\xi\xi 0]$ phonon softening and the martensitic transformation, which occurs in Fe-rich ordered Fe–Pt. We find that the $TA_1[\xi\xi 0]$ phonon softening, especially at the M-point zone boundary, does not depend on the composition of the investigated crystals. In $Fe_{74.5}Pt_{25.5}$, however, the antiferrodistortive phase transition temperature is enhanced due to tetragonal strain preceding the martensitic transition. In $Fe_{77}Pt_{23}$ a precursor driven premartensitic phase transition is not observed. The structure of the martensite is, however, influenced by the soft mode lattice instability of the austenite. This would explain the origin of structural details found previously for Fe_3Pt thermoelastic martensite.

PACS. 63.20.Dj Phonon states and bands, normal modes, and phonon dispersion – 81.30.Kf Martensitic transformations – 61.12.-q Neutron diffraction and scattering

1 Introduction

In a previous publication (paper I) [1] we have reported about neutron scattering results on the $TA_1[\xi\xi 0]$ phonon dispersion of two $Fe_{72}Pt_{28}$ crystals, one disordered fcc, the other well ordered in the Cu_3Au ($L1_2$) structure. In both crystals, softening of the transverse acoustic phonons propagating in [110] direction with polarisation along $[1\bar{1}0]$ was detected on cooling below the Curie temperatures of the ferromagnetic Invar alloys. In disordered $Fe_{72}Pt_{28}$, the softening is found maximum for long wave phonons near the zone center, quite similar as in other Fe-rich fcc Invar alloys Fe–Ni and Fe–Pd. In ordered $Fe_{72}Pt_{28}$, long wave phonon softening is present as well. In addition, however, a soft phonon mode develops at the M-point zone boundary, dominating the whole $TA_1[\xi\xi 0]$ phonon branch of ordered $Fe_{72}Pt_{28}$ at low temperatures and leading to an antiferrodistortive phase transition below about 50 K.

For ordered $Fe_{72}Pt_{28}$, the change of the structure at low temperatures is described by the condensed M_4-mode; a rotation of octahedra built up by neighboring Fe-atoms of the $L1_2$-structure around one of the [100] axes. Anomalous enhancement of the high and low field magnetization [2,3] as well as of the atomic volume [4] in the low temperature state suggest that the $TA_1[\xi\xi 0]$ phonon softening arises from magnetovolume coupling, *i.e.* from the Invar effect in ordered $Fe_{72}Pt_{28}$. Both the enlargement of the Fe-magnetic moment and of the atomic volume is apparently achieved by symmetry reduction in the low temperature phase, which is consistent with the microscopic theory of the Invar effect [5]. The phase transition resembles those observed in the perovskites, *e.g.* in incipient ferroelectric $SrTiO_3$.

With the increase of the Fe-content, both disordered fcc and $L1_2$ ordered Fe–Pt alloys become increasingly unstable against the martensitic transformation into a bct or bcc lattice. The M_S start temperature of this transition strongly depends on composition and degree of atomic order. Ultrasonic [6,7] and neutron scattering [8] experiments on Fe–Pt Invar alloys have shown significant softening especially of the shear elastic constant C' and of the corresponding long wavelength $TA_1[\xi\xi 0]$ phonon modes, indicating the tendency of the cubic lattice to lower symmetry in the ferromagnetic state by homogeneous or long wave modulated tetragonal strain. Indeed, disordered and ordered Fe-rich Fe–Pt alloys have been reported to exhibit the fct phase at low temperatures within a narrow range of composition close to the bct phase boundary [9–11] or even in coexistence with the bct martensite [9].

[a] e-mail: kaestner@ttphysik.uni-duisburg.de

Beyond the homogeneous or long wavelength shear, phonon softening in the Fe-Invar alloys as a dynamical precursor of the martensitic transition is not established. Static precursors of the martensitic transition in the Fe–Pd and Fe–Pt Invar alloys have been manifested, so far, by X-ray, electron, and neutron diffraction as tetragonally strained defect structures growing in the austenite approaching the martensitic transition [9–12]. Structural details observed in the thermoelastic martensite of a well ordered $Fe_{76}Pt_{24}$ alloy [13] suggest, however, that this martensite might be generated by shear and shuffle as well, like in many other ordered martensitic materials [14,15].

In the present paper we report on neutron scattering results obtained for two ordered Fe-rich Fe–Pt single crystals: $Fe_{74.5}Pt_{25.5}$ and $Fe_{77}Pt_{23}$. The crystal containing 25.5 at.% Pt is very close to the martensitic transition ($M_S \approx 0$ K). The crystal containing 23 at.% Pt transforms into bct martensite below $M_S \approx 210$ K. For both crystals, we have investigated the premartensitic $TA_1[\xi\xi 0]$ phonon softening, especially that of the soft zone boundary mode, and the elastic scattering along the [110] direction. The results are compared with those obtained for ordered $Fe_{72}Pt_{28}$. We discuss the role of the acoustic phonon softening both at the zone center and at the M-point zone boundary in relation to the observed premartensitic and martensitic changes of the structure.

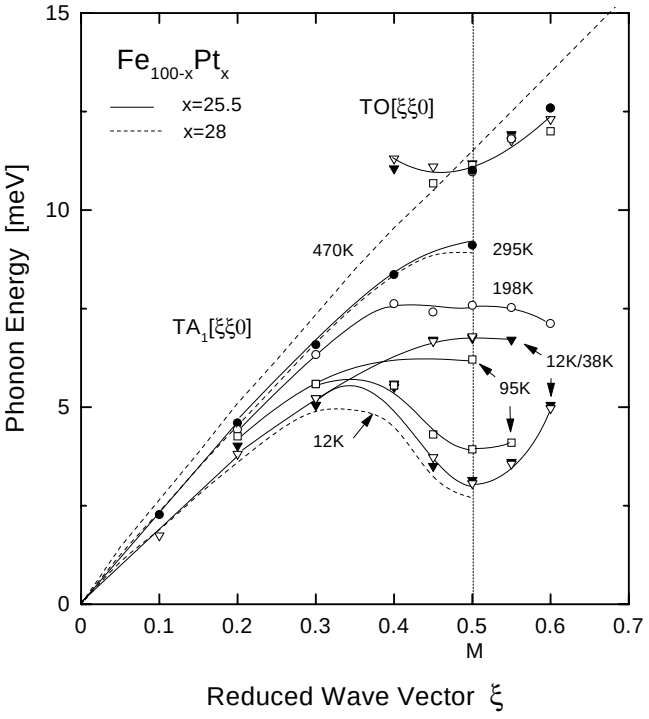

Fig. 1. $TA_1[\xi\xi 0]$ phonon branch and lowest $TO[\xi\xi 0]$ phonon branch near zone boundary of ordered $Fe_{74.5}Pt_{25.5}$ at different temperatures. Data of $Fe_{72}Pt_{28}$ at 470 K and 12 K are included for comparison.

2 Experiment

Two Fe–Pt crystals of 2 to 3 cm length and 1 cm diameter containing nominally 23 at.% and 25.5 at.% Pt have been prepared by a Bridgman method and ordered in the $L1_2$ structure as described in paper I. As for $Fe_{72}Pt_{28}$, concentration and homogeneity was checked by energy dispersive X-ray investigation to agree with the nominal value within ±1 at.%. Taking rocking curves through the (220) reflection with neutrons gave mosaic spreads of 2.4° and 3° (fwhm) for the crystals with 25.5 at.% Pt and 23 at.% Pt, respectively. This mosaic spread, which is larger than that determined for the previously investigated $Fe_{72}Pt_{28}$ crystals (0.4°), is partly ascribed to premartensitic strains and defects, developing even at elevated temperatures in the presently investigated crystals. According to the phase diagram of Fe–Pt in the vicinity of Fe_3Pt (see Fig. 6), a concentration fluctuation of 1 at.% Pt on a sufficiently large length scale would result in the change of M_S by ≈ 100 K.

Elastic and inelastic neutron scattering was performed with the 1T1 three-axis spectrometer, installed at the Orphée reactor, Laboratoire Léon Brillouin, CEA-CNRS, Saclay. Pyrolitic graphite crystals were used as monochromator (vertical focusing) and analyser (horizontal focusing). For all measurements a constant final wave vector $k_f = 2.662$ Å^{-1} or 3.840 Å^{-1} was used. Different acoustic phonon dispersions along high symmetry directions were determined mainly by taking constant q-scans at various temperatures between 295 K and 12 K. The $TA_1[\xi\xi 0]$ phonon branch was measured mainly between the (220) and (310) Bragg reflection within the (001) scattering plane. The phonon energies were determined by fitting damped oscillator functions to the cross sections taking into account the resolution function of the spectrometer.

3 Results and discussion

3.1 $TA_1[\xi\xi 0]$ phonon dispersion

As already reported for $Fe_{72}Pt_{28}$, we observed that among the acoustic phonon modes investigated in the high symmetry directions only the $TA_1[\xi\xi 0]$ modes considerably soften with decreasing temperature below the magnetic Curie temperature T_C. Therefore, we restrict our discussion about the dynamical behaviour of the Fe–Pt crystals on the ξ-dependence of the $TA_1[\xi\xi 0]$ modes and on their dependence on temperature and composition.

In Figure 1, the $TA_1[\xi\xi 0]$ phonon branch and part of the lowest transverse optical branch near the zone boundary of $Fe_{74.5}Pt_{25.5}$ ($T_C \approx 455$ K) are shown for different temperatures between 12 K and 295 K. The high and low temperature phonon branches of ordered $Fe_{72}Pt_{28}$ ($T_C \approx 500$ K) have been added for direct comparison. We note first that at 470 K, the highest measuring temperature for $Fe_{72}Pt_{28}$, no splitting could be observed within the resolution of the spectrometer between the acoustic and optical branch at the M-point. These modes are apparently almost degenerate at temperatures close to and above T_C. Comparing the ξ-dependence of the $TA_1[\xi\xi 0]$

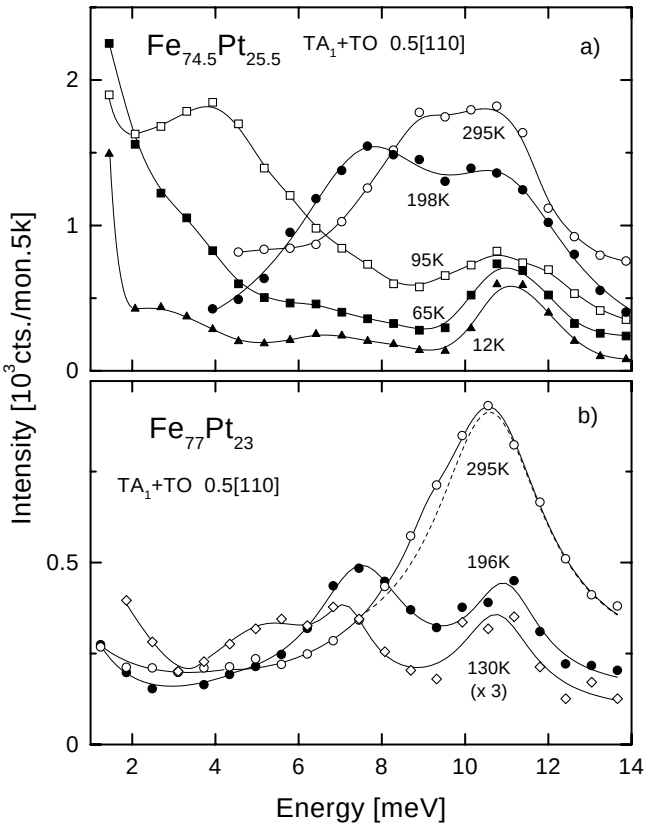

Fig. 2. TA_1 and TO 0.5[110] phonon scattering cross sections for a) $Fe_{74.5}Pt_{25.5}$ and b) $Fe_{77}Pt_{23}$ at different temperatures. Cross section of $Fe_{77}Pt_{23}$ at 130 K is enlarged by factor 3 above background. Dotted curve denotes fit to the optical phonon cross section at 295 K.

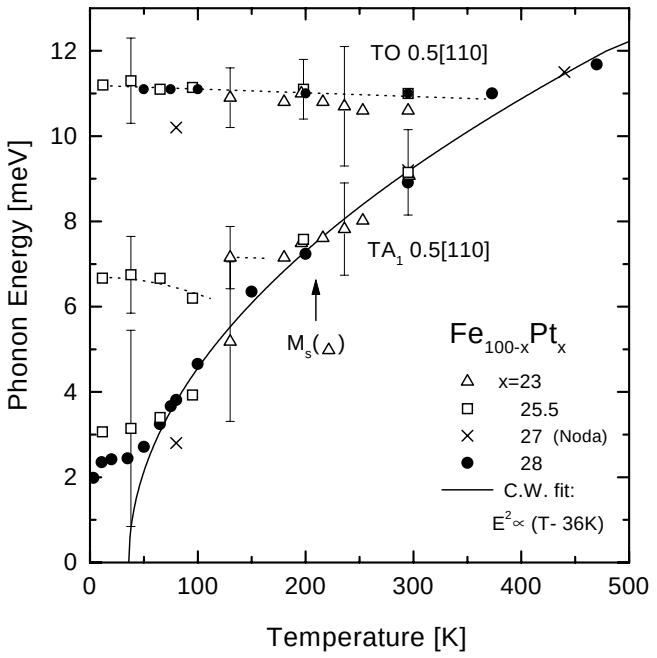

Fig. 3. TA_1 and TO 0.5[110] phonon energies *vs.* temperature for ord. Fe–Pt crystals. Data for $Fe_{73}Pt_{27}$ are taken from reference [16]. Vertical bars denote typical widths of cross sections. Solid curve denotes Curie-Weiss fit. Dotted lines are guide to the eyes.

phonon dispersions of both crystals at room temperature and at 12 K, we ascertain a very similar behaviour. The phonon energies along the whole acoustic branch decrease with decreasing temperature, the decrease is pronounced near and right at the zone boundary. This contrasts the behaviour of the lowest zone boundary optical branch which is almost temperature independent.

Whereas for both crystals the lowest zone boundary acoustic phonon energies at 12 K are the same within the errors of the measurements, for $Fe_{74.5}Pt_{25.5}$, roughly below 100 K, two phonon energies can be fitted to the cross sections determined near the M-point. This can be inferred from Figure 2a, where for $Fe_{74.5}Pt_{25.5}$ some of the zone boundary phonon spectra measured at different temperatures are plotted. As this figure shows, the optical phonon cross sections near 11 meV do essentially not change with decreasing temperature. The acoustic ones, however, are shifted to low energies, become rather broadened below $\sim$ 100 K, and exhibit a double peak profile at lower temperatures. This behaviour clearly differs from that observed in $Fe_{72}Pt_{28}$. Furtheron, the cross section of the acoustic zone boundary mode in $Fe_{74.5}Pt_{25.5}$ rapidly decreases on cooling the crystal below 100 K. Simultaneously, the intensity of the elastic scattering at the M-point increases (see Fig. 4).

In Figure 2b, the zone boundary phonon cross sections of $Fe_{77}Pt_{23}$ determined at 295 K, 196 K and 130 K are shown. At 295 K, not far below $T_C \approx 350$ K of this crystal, the cross section of the acoustic mode is rather small, as compared with that of $Fe_{74.5}Pt_{25.5}$, and almost obscured by that of the optical mode. The dashed line in Figure 2b denotes a fit to the dominating optical mode. The energy of the acoustic mode is, however, identical to that of $Fe_{74.5}Pt_{25.5}$. Even at 196 K, close below the start temperature of the martensitic transformation $M_S \approx 210$ K, the mode energies for both crystals are the same, indicating that at this temperature the zone boundary phonon softening in the remaining austenite is essentially independent of the martensite formation. A similar behaviour could be traced in this crystal down to temperatures of about 130 K, until most of the austenite had transformed. Figure 2b shows that at 130 K, the phonon cross section of $Fe_{77}Pt_{23}$ exhibits a double peak profile in the range between 4 and 8 meV similar to that found for $Fe_{74.5}Pt_{25.5}$ at lower temperatures.

In Figure 3, the energies of the $TA_1$0.5[110] and of the lowest optical M-point zone boundary phonon modes are plotted *vs.* temperature for all investigated ordered Fe–Pt crystals including also the data reported by Noda and Endoh for $Fe_{73}Pt_{27}$ [16]. Vertical bars set symmetrically around some phonon energies indicate the width of the corresponding cross sections to illustrate the damping of the modes. The dotted lines are guide to the eyes,

whereas the solid curve represents the Curie-Weiss fit to the squared mode energy of $Fe_{72}Pt_{28}$.

The data in Figure 3 suggest that at high temperatures, especially above the Curie temperatures of the investigated crystals, the optical and acoustic zone boundary modes are almost degenerate. To clarify the incipient softening of the transverse acoustic zone boundary mode, a more detailed neutron scattering study at high temperatures and comparison with corresponding magnetization data would be necessary and helpful, respectively. We note that normal quasi harmonic behaviour of the zone boundary phonon modes is expected well above T_C. This has been actually found for the low-ξ TA_1 modes in Fe_3Pt [8] and for the elastic constant C' [6].

Furthermore, Figure 3 reveals that in the temperature range between about 150 K and 300 K the acoustic zone boundary mode energy is essentially the same for all investigated Fe–Pt crystals, irrespective of their quite different Curie temperatures, ranging from 350 K to above 500 K. Apparently, not the Curie temperature but the temperature dependent spontaneous magnetization determines the softening of the phonon modes of the alloys. For Fe–Pt, the mean magnetic moment of the Fe-atoms increases with increasing Fe-content, whereas T_C decreases. The spontaneous magnetization, *e.g.* at 200 K [4], varies, therefore, much less with composition than T_C.

At temperatures roughly below 150 K, the phonon modes of $Fe_{72}Pt_{28}$ and $Fe_{74.5}Pt_{25.5}$ differ with respect to their scattering profiles (compare *e.g.* Fig. 2a with Fig. 4 of paper I). The lower phonon energy of $Fe_{74.5}Pt_{25.5}$ exhibits a temperature dependence similar to that of $Fe_{72}Pt_{28}$, namely the deviation from the Curie Weiss behaviour towards a roughly constant value between 2 and 3 meV below about 50 K. We conclude that this low energy mode of $Fe_{74.5}Pt_{25.5}$ reflects the behaviour inherent in the zone boundary mode softening like in $Fe_{72}Pt_{28}$. The mode with the higher energy between 6 and 7 meV is considered as the dynamical response from defect regions within the crystal (see our discussion further below).

3.2 Elastic scattering

Figure 4 shows some data of the diffuse elastic scattering, actually measured along $[1\bar{1}0]$ between the (200) and $(3\bar{1}0)$ Bragg reflections for $Fe_{72}Pt_{28}$ and between the (220) and (310) Bragg reflections for $Fe_{74.5}Pt_{25.5}$ and $Fe_{77}Pt_{23}$. On the left side of the figure, the intensity contours are plotted on a log scale *vs.* the reduced wave vector ξ for high and low temperatures, respectively. On the right side, the temperature dependence of the scattering intensities at the zone boundary ($\xi = 0.5$) and near the zone center ($\xi = 0.1$ or 0.2) is shown. Intensity numbers given in the middle and the lower row are directly comparable to each other. Those given in the upper row, which have been obtained on a different spectrometer, are comparable to the others within the order of magnitude.

For $Fe_{72}Pt_{28}$ (upper row), the elastic scattering intensity increases on cooling mainly at $\xi = 0.5$ and below

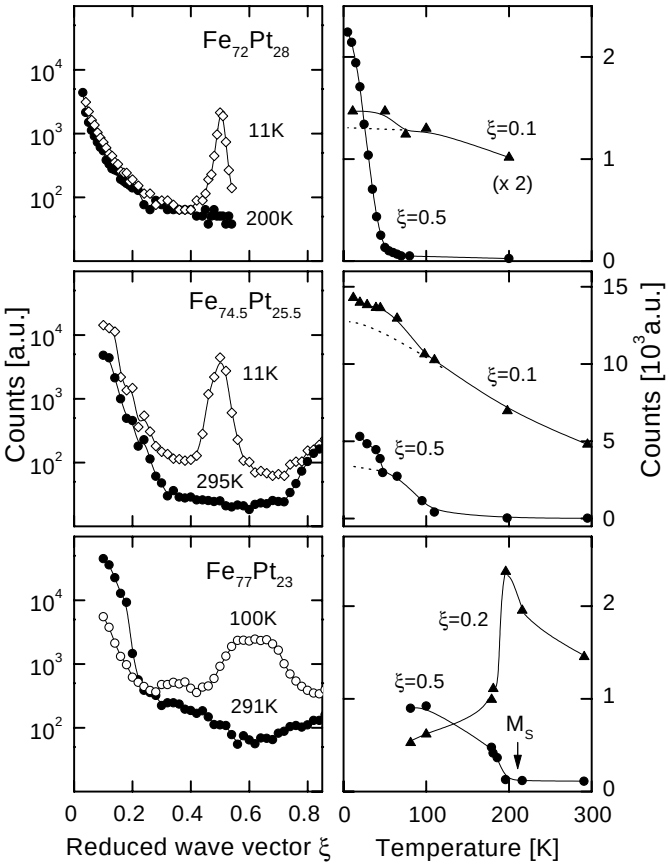

Fig. 4. Elastic scattering intensities along $TA_1[\xi\xi 0]$ phonon branch for $Fe_{72}Pt_{28}$, $Fe_{74.5}Pt_{25.5}$ and $Fe_{77}Pt_{23}$ at high and low temperatures. Left side: on log. scale *vs.* reduced wave vector ξ; Right side: on lin. scale for $\xi = 0.1(0.2)$ and $\xi = 0.5$ *vs.* temperature. Full lines are guides to the eyes, dotted lines are extrapolations of the temperature dependences.

about 50 K, indicating the development of the superstructure peak, well localized in q-space and corresponding to the temperature where the soft mode energy levels off to approach a constant value (see Fig. 3 and paper I). For this crystal, at $\xi = 0.1$, in the vicinity of the (200) Bragg peak, the scattering intensity increases only weakly on cooling from 200 K to 11 K. Note the enlargement by the factor 2 in the figure. Extrapolation of the high temperature behaviour, indicated by the dotted line in the upper right panel of Figure 4, suggests a slight enhancement of the scattering at $\xi = 0.1$ below 50 K, which is also found for smaller ξ-values. It likely originates from strain related to the zone boundary transformation. We suspect that the low temperature antiferrodistortive transformation is accompanied by a small change of the c/a ratio of the cubic lattice ($c/a < 1$). X-ray investigations performed by us on polycrystals with similar composition and degree of atomic order did, however, so far, not yield conclusive results on the low temperature structure.

The elastic scattering of $Fe_{74.5}Pt_{25.5}$, shown in the middle row of Figure 4, differs markedly from that of $Fe_{72}Pt_{28}$. First, the intensity at small ξ is much larger than that of $Fe_{72}Pt_{28}$, consistent with the larger mosaic

spread of $Fe_{74.5}Pt_{25.5}$. Measurement of the intensity contours taken near the (220) Bragg reflection of this crystal at room temperature yield a streak along the $[1\bar{1}0]$ direction extending into the Brillouin zone to about $\xi = 0.3$. Similar streaks in the elastic scattering contours have been observed in a number of alloys as typical precursors of a first order structural phase transformation in combination with mode softening [17]. This Huang type scattering originates from local structural defects of the cubic lattice, characterized by the shear strain of the (110) planes along the $[1\bar{1}0]$ direction, which is favoured by a small elastic constant C' and by small $TA_1[\xi\xi 0]$ phonon energies. A proper combination of such shears transforms the fcc- into the fct-lattice. As shown in Figure 4, the defect scattering at small ξ considerably increases on cooling the $Fe_{74.5}Pt_{25.5}$ crystal from ambient to low temperatures, *i.e.* by a factor 3 within the whole ξ-range up to $\xi \approx 0.3$. Apparently, the number of the fct-lattice like defects is growing with decreasing temperature, *i.e.* approaching the martensitic transformation. The behaviour is similar to that of disordered $Fe_{72}Pt_{28}$, reported in paper I, both crystals having about the same Martensite start temperature $M_S \approx 0$ K.

Like ordered $Fe_{72}Pt_{28}$, the $Fe_{74.5}Pt_{25.5}$ crystal also exhibits the M-point superstructure peak at low temperatures. The data, plotted for $\xi = 0.5$ on the right side of the middle row of Figure 4, suggest, that the zone boundary transformation of this crystal occurs in two steps as indicated by the dotted line. In a first step, the peak at $\xi = 0.5$ starts to develop with decreasing temperature below about 110 K. This is roughly the temperature at which the phonon branch near and right at the zone boundary apparently splits (*cf.* Fig. 3). We consider this transformation as induced by the local fct defects. In a second step, below about 50 K, the elastic scattering increases more steeply on further cooling. We note that this behaviour is similar to that observed in $Fe_{72}Pt_{28}$, namely the appearance of the superstructure peak coinciding with the deviation of the corresponding phonon frequencies from the Curie Weiss like softening. Again, similar to the elastic scattering in $Fe_{72}Pt_{28}$, the scattering at small ξ in $Fe_{74.5}Pt_{25.5}$ seems to be clearly enhanced by the zone boundary transition, as indicated by another dotted line for $\xi = 0.1$ in Figure 4.

From the mutual dependence of zone boundary and zone center strain and from the temperature dependence of the zone boundary mode energies in $Fe_{74.5}Pt_{25.45}$ we derive the following view: Apparently, locally fct-strained regions exist in this crystal which – according to the composition – have a much higher density than those in $Fe_{72}Pt_{28}$. They grow with respect to their number and spatial extension with decreasing temperature, approaching the martensitic transition ($M_S \approx 0$ K) and induce the structural transformation corresponding to the soft zone boundary phonons. In those local regions of the lattice, where the c/a ratio $r < 1$ is smaller than a critical value, the Fe-octahedrons are rotated around the c-axis away from their symmetric positions, corresponding to the intrinsic instability of the cubic lattice. Consequently, the structure in $Fe_{74.5}Pt_{25.45}$ is considered to change heterogeneously with decreasing temperature: Those zone boundary phonon modes which stem from the defect lattice constitute the upper part of the splitted phonon branch with nearly constant energy below ~ 120 K (see Fig. 3). The other modes, stemming from the untransformed cubic lattice, constitute the lower branch. They continue to soften with decreasing temperature until the lattice gets intrinsically unstable, here below about 50 K.

To emphasize the relevance of structural defects with respect to the martensitic transformation we add some short remarks on the possible origin of the embryonic like fct distorted regions and their development with the decrease of temperature. Seeds of the low temperature fct, bct or bcc martensitic phase might be stable even at very high temperatures in fcc Fe_3Pt due to local concentration fluctuations. These fluctuations locally change the number and the atomic volume of neighboring Fe atoms, which are considered as critical parameters for the Fe-magnetic moment and for the structural stability [18]. The defects may survive even in a well ordered $L1_2$-structure of a single crystal due to short range disorder prevailing at low temperatures, *e.g.* at anti-site atoms due to off-stoichiometry and at anti-phase boundaries. It is mentioned in this context that extended X-ray absorption fine structure measurements (EXAFS) in o. $Fe_{74}Pt_{26}$ [19] have shown that the nearest neighbor Pt-Fe and the Pt-Pt defect pair distances differ by about 2% and that both change anomalously on the decrease of the temperature below about 100 K.

Finally, we discuss the corresponding elastic scattering data of the $Fe_{77}Pt_{23}$ crystal, shown in the lower row of Figure 4. At room temperature, the scattering near $\xi = 0.1$ from this crystal is even larger than that from the crystal discussed before and hardly varies with decreasing temperature above M_S. Therefore, on the right hand side of the lower row in Figure 4, the scattering intensity at $\xi = 0.2$ is plotted *vs.* temperature. It strongly increases on cooling the crystal due to the increase of local strain, especially near M_S, until below about 200 K $< M_S \approx 210$ K, it steeply diminishes indicating the martensitic transformation of the majority of the crystal into a bct lattice (see below). On this transition, near the M-point of the austenitic lattice, the scattering rapidly increases with decreasing temperature. Since the M-point of the austenite lattice is not considered as a zone boundary or symmetry point of the bct lattice (see *e.g.* Fig. 5), it is not surprising that this scattering is shifted and rather spread along the $[1\bar{1}0]$ direction. Scanning along the [110] direction through this M-point, the scattering intensity was found rather modulated within the (001) plane of the austenite.

Though the scattering from the martensite cannot be clearly related to a specific structural change like in the austenite, *i.e.* to a rotational displacement of the Fe-atoms, we strongly suggest that a similar transition occurs in the martensite. Electron microscopy studies on the bct martensite of a well ordered $Fe_{76}Pt_{24}$ alloy have revealed reflections corresponding to a shuffle movement of the Fe-atoms away from the high symmetry positions, *i.e.*

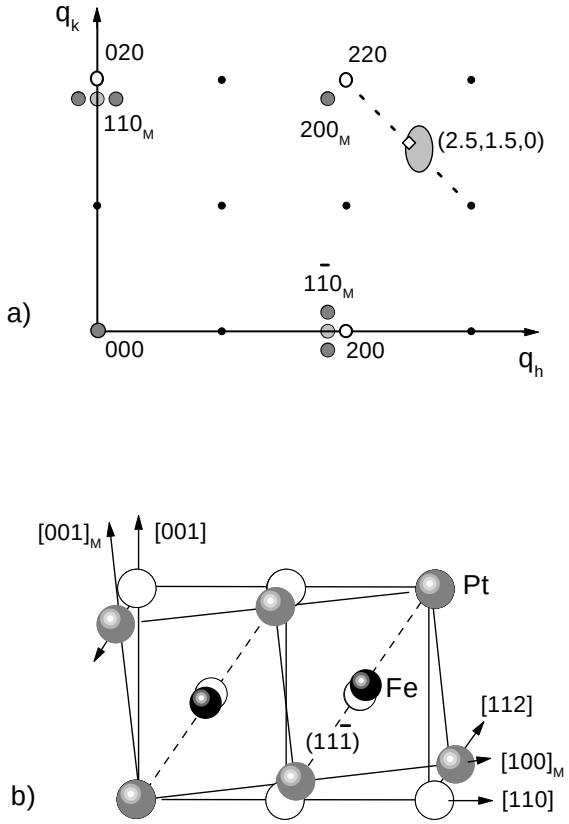

Fig. 5. (a) Bragg-reflections on (001)-scattering plane of $Fe_{77}Pt_{23}$ austenite and projected bct-martensite reflections indexed in Bain correspondence including scattering contour found for martensite near M-point (2.5,1.5,0) (schematic). (b) lattice model according to Figure 5a.

the face centers of the austenite lattice. Possibly, even the electronic structure within a bct lattice of ordered Fe_3Pt favours such a displacement.

3.3 Martensitic transformation

The martensitic transformation of the $Fe_{77}Pt_{23}$ crystal was traced by several elastic scans through and close to the (200), (020), (220), and $(\bar{1}1\bar{1})$ Bragg reflections at different temperatures near and below M_S. From the appearance of intensities growing at new fixed positions in q-space with decreasing temperature at the expense of the austenite, we determined $M_S \approx 210$ K and identified the martensite basically consisting of a bct lattice in a Bain correspondence to the austenite. The positions of the new Bragg reflections found in the vicinity of the (001) scattering plane of the austenite and projected on this plane are shown schematically in Figure 5a, together with the location of scattering intensity determined near the (2.5,1.5,0) M-point below M_S. Correspondingly, in Figure 5b, the cells of one bct-lattice variant are sketched projected on the $(1\bar{1}0)$ austenite lattice plane. The lattice parameters determined for the austenite are: $a(300\text{ K}) = 3.750$ Å; $a(M_S) = 3.735$ Å; and those for the bct-martensite: $a = 2.864$ Å, $c = 3.175$ Å, $c/a = 1.109$, the latter being independent of the temperature within the resolution of the measurements. The volume change at M_S is $\Delta V/V = -0.4\%$. These values are in very good agreement with lattice parameters reported for the bct-martensite of ordered $Fe_{76}Pt_{24}$ [20] and partially ordered $Fe_{75}Pt_{25}$ [11].

Observing the reverse transformation with increasing temperature by comparing the intensities of a (200) bct and a (220) fcc Bragg reflection located close together within the austenitic (001) scattering plane, we conclude that at M_S (apparently) only less than half of the martensite had re-transformed to austenite within the original orientation and even at room temperature a small amount of martensite was retained. Thus, the martensitic transition observed in this crystal is not considered as thermoelastic. In addition, at 300 K, the scattering intensity at the position of the austenite $(\bar{1}1\bar{1})$ Bragg reflection and evidently single crystallinity was lost.

From the positions of the splitted Bragg reflections of the bct-martensite, we infer that the transformation of the parent into the product phase is mediated mainly by the typical (111) $[11\bar{2}]$ type shear strain (see Fig. 5b). The resistance against this shear, *i.e.* the relevant elastic constant $C = (2C' + C_{44})/3$ is low if C' is small. This has been verified for partially ordered $Fe_{75}Pt_{25}$ [21]. For our crystals investigated, a softening comparable to that of the elastic constant C' is found for the low-ξ $TA_1[\xi\xi 0]$-phonons above the M_S temperature. For $Fe_{77}Pt_{23}$, a reduction of the phonon energy at $\xi = 0.2$ and $T \approx M_S$ by about 20% relative to the room temperature value is determined. This roughly compares with the phonon softening at $\xi = 0.2$ for $Fe_{74.5}Pt_{25.5}$ between room temperature and $M_S \approx 0$ K. For a direct comparison with the elastic constant C', however, more precise data of phonon energies in the low-ξ region ($\xi < 0.1$) are necessary.

4 Summary and conclusions

We have shown that the investigated ordered Fe–Pt crystals exhibit considerable softening of the whole $TA_1[\xi\xi 0]$ phonon branch below the Curie temperature. Pronounced softening is found at the M-point zone boundary, as previously determined for $Fe_{72}Pt_{28}$.

To summarize our results on the phonon dynamics and on the related structural changes observed in the investigated Fe-rich Fe–Pt alloys, we show in Figure 6 the magnetic and structural phase diagram of ordered Fe–Pt in the range between 21 and 30 at.% Pt. Special interest is focused on the tetragonal phase at low temperatures. This phase has been identified and established by our work as due to the $TA_1 0.5[110]$ phonon instability. It is characterized by a displacement of the Fe-atoms away from their symmetric positions in the $L1_2$-structure and by a doubling of the lattice unit cell. At compositions near $Fe_{72}Pt_{28}$, the tetragonal phase is intrinsically stable below about 50 K (dashed line in Fig. 6). With the increase of the Fe-content and with the approach to the martensitic phase, the boundary between the tetragonal and the cubic $L1_2$-phase is shifted to higher temperatures due to the

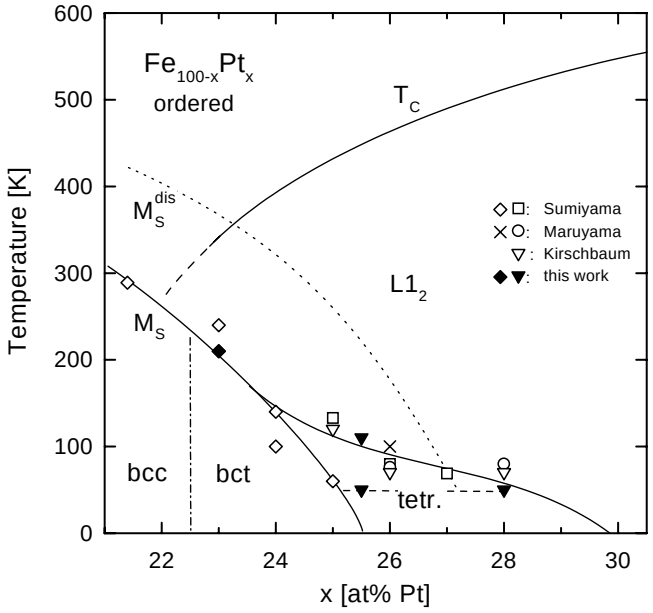

Fig. 6. Magnetic and structural phase diagram of ordered $Fe_{100-x}Pt_x$ for $21 < x < 30$ at.% Pt. Data of T_C, M_S, M_S^{dis} (for disordered Fe–Pt) and boundary between $L1_2$ and tetragonal phase are from references [2–4, 19] and present work.

increasing premartensitic (zone center) tetragonal strain. This strain is considered to originate from local fct like lattice defects within the ordered structure of the austenite. It may become relevant at temperatures near or even above the M_S temperature of the disordered fcc phase, marked in Figure 6 by a dotted curve.

From the measurements on ordered $Fe_{77}Pt_{23}$ we have found that the $TA_1 0.5[110]$-zone boundary phonon softening in the austenite is rather unaffected by the martensitic transition into a bct lattice, starting below about 210 K. From the Bragg positions of the martensite, we infer that the homogeneous shear strain is the important element within the kinetics of this transformation. It is influenced by the softness of the elastic constant C' and of the low-ξ transverse acoustic phonons. Diffuse elastic scattering from the martensite suggests, however, that the zone boundary structural instability is preserved in the martensite. This may be even more pronounced and important in alloys with compositions very close to Fe_3Pt, where the tetragonal phase is intermediate between the $L1_2$-austenite and the thermoelastic bct-martensite.

As a final conclusion we shortly address ourselves to the question about the general role of phonon softening as dynamical precursor of the martensitic phase transformation. Our present results and those obtained for the other Fe-rich fcc alloys, both experimentally and theoretically, suggest that the martensitic transformation, as manifesting in the strong composition dependence of the M_S temperature, is of electronic origin and not primarily controlled by soft phonons. The latter are, however, relevant for the formation and symmetry of premartensitic phases. As we have shown for the ordered Fe–Pt system in the vicinity of the martensitic phase boundary, the premartensitic cubic to tetragonal lattice transformation may comprise a combination of strains related to different soft $TA_1[110]$ phonons. Moreover, our results suggest that these soft phonons influence also the morphology of the martensitic lattice on microscopic length scale, at least in the case when the martensite forms at low enough temperatures.

Partial support of this work by the HCM Program of the European Community (No. ERB CHGECT 920001) and Deutsche Forschungsgemeinschaft within SFB 166 is kindly acknowledged.

References

1. J. Kästner, W. Petry, S.M. Shapiro, A. Zheludev, J. Neuhaus, Th. Roessel, E.F. Wassermann, H. Bach (accepted for publication in EPJ B).
2. H. Maruyama, J. Phys. Soc. Jap. **55**, 2834 (1986).
3. U. Kirschbaum, thesis, Gerhard Mercator University Duisburg, 1996.
4. K. Sumiyama, Y. Emoto, M. Shiga, Y. Nakamura, J. Phys. Soc. Jap. **50**, 3296 (1981).
5. P. Entel, E. Hoffmann, P. Mohn, K. Schwarz, V.L. Moruzzzi, Phys. Rev. B **47**, 8706 (1993).
6. G. Hausch, J. Phys. Soc. Jap. **37**, 819 (1974).
7. H.C. Ling, W.S. Owen, Acta metall. **31**, 1343 (1983).
8. K. Tajima, Y. Endoh, Y. Ishikawa, W.G. Stirling, Phys. Rev. Lett. **37**, 519 (1976).
9. S. Muto, R. Oshima, F.E. Fujita, Met. Trans. **19A**, 2723 (1988).
10. M. Foos, C. Frantz, M. Gantois, Scripta Metall. **12**, 795 (1978).
11. M. Matsui, K. Adachi, H. Asano, Sci. Rep. RITU A **29**, Suppl. 1, 61 (1981).
12. H. Seto, Y. Noda, Y. Yamada, J. Phys. Soc. Jap. **59**, 965, 978 (1990).
13. T. Tadaki, Y. Nakata, K. Shimizu, Mat. Sci. Forum **56-58**, 169 (1990).
14. S.M. Shapiro, Mat. Sci. Forum **56-58**, 33 (1990).
15. W. Petry, J. Phys. IV France **5**, C2-15 (1995).
16. Y. Noda, Y. Endoh, J. Phys. Soc. Jap. **57**, 4225 (1988).
17. S.M. Shapiro, B.X. Yang, Y. Noda, L.E. Tanner, D. Schryvers, Phys. Rev. B **44**, 9301 (1991).
18. M. Schröter, H. Ebert, H. Akai, P. Entel, E. Hoffmann, G.G. Reddy, Phys. Rev. **52**, 188 (1995).
19. H. Maruyama, K. Shirai, H. Maeda, W.L. Liu, L.O. Yamada, J. Phys. Soc. Jap. **56**, 4377 (1987).
20. T. Tadaki, K. Shimizu, Scripta Metall. **9**, 771 (1975).
21. W. S. Owen, Mater. Sci. Eng. A **127**, 19 (1990).